Diabetologia (2011) 54:2347–2357
DOI 10.1007/s00125-011-2221-6

ARTICLE

Deletion of *Ia-2* and/or *Ia-2β* in mice decreases insulin secretion by reducing the number of dense core vesicles

T. Cai · H. Hirai · G. Zhang · M. Zhang · N. Takahashi · H. Kasai · L. S. Satin · R. D. Leapman · A. L. Notkins

Received: 10 December 2010 / Accepted: 23 May 2011 / Published online: 6 July 2011

Abstract
Aims/hypothesis Islet antigen 2 (IA-2) and IA-2β are dense core vesicle (DCV) transmembrane proteins and major autoantigens in type 1 diabetes. The present experiments were initiated to test the hypothesis that the knockout of the genes encoding these proteins impairs the secretion of insulin by reducing the number of DCV.
Methods Insulin secretion, content and DCV number were evaluated in islets from single knockout (*Ia-2* [also known as *Ptprn*] KO, *Ia-2β* [also known as *Ptprn2*] KO) and double knockout (DKO) mice by a variety of techniques including electron and two-photon microscopy, membrane capacitance, Ca^{2+} currents, DCV half-life, lysosome number and size and autophagy.
Results Islets from single and DKO mice all showed a significant decrease in insulin content, insulin secretion and the number and half-life of DCV ($p<0.05$ to 0.001). Exocytosis as evaluated by two-photon microscopy, membrane capacitance and Ca^{2+} currents supports these findings. Electron microscopy of islets from KO mice revealed a marked increase ($p<0.05$ to 0.001) in the number and size of lysosomes and enzymatic studies showed an increase in cathepsin D activity ($p<0.01$). LC3 protein, an indicator of autophagy, also was increased in islets of KO compared with wild-type mice ($p<0.05$ to 0.01) suggesting that autophagy might be involved in the deletion of DCV.
Conclusions/interpretation We conclude that the decrease in insulin content and secretion, resulting from the deletion of *Ia-2* and/or *Ia-2β*, is due to a decrease in the number of DCV.

Keywords Autophagy · Capacitance · Dense core vesicle · Diabetes · Electron microscopy · Gene knockout · Insulin · Pancreatic islet · Protein tyrosine phosphates · Two-photon microscopy

Abbreviations
DCV Dense core vesicle
DKO Double knockout
KO Knockout

T. Cai and H. Hirai contributed equally to this study.

Electronic supplementary material The online version of this article (doi:10.1007/s00125-011-2221-6) contains peer-reviewed but unedited supplementary material, which is available to authorised users.

T. Cai (✉) · H. Hirai · A. L. Notkins (✉)
Experimental Medicine Section, Oral Infection and Immunity Branch, National Institute of Dental and Craniofacial Research (NIDCR), National Institutes of Health (NIH),
Bethesda, MD 20892, USA
e-mail: tcai@mail.nih.gov

A. L. Notkins
e-mail: anotkins@dir.nidcr.nih.gov

G. Zhang · R. D. Leapman
Laboratory of Bioengineering and Physical Science, National Institute of Biomedical Imaging and Bioengineering, NIH,
Bethesda, MD, USA

M. Zhang · L. S. Satin
Department of Pharmacology and Toxicology,
Virginia Commonwealth University,
Richmond, VA, USA

N. Takahashi · H. Kasai
Laboratory of Structural Physiology, Center for Disease Biology and Integrative Medicine, University of Tokyo,
Tokyo, Japan

L. S. Satin
Department of Pharmacology and Brehm Diabetes Center,
University of Michigan Medical School,
Ann Arbor, MI, USA

IA-2 Islet antigen 2
SKO Single knockout

Introduction

Islet antigen 2 (IA-2) and IA-2β are major autoantigens in type 1 diabetes [1–3]. Autoantibodies to these two proteins appear years before the development of clinical disease and in combination with autoantibodies to the autoantigens glutamic acid decarboxylase 65 and insulin have become important diagnostic and predictive biomarkers [3]. Population screening showed that individuals with autoantibodies to two or more of these major autoantigens are at a 50% or greater risk of developing type 1 diabetes within 5 years [4–6].

Detailed studies on the properties of IA-2 and IA-2β (also known as ICA512 and phogrin, respectively) revealed that they are integral transmembrane proteins of dense core vesicles (DCV) and widely distributed in neuroendocrine cells throughout the body (e.g. pancreatic islets, adrenals, brain) [7, 8]. Both are members of the protein tyrosine phosphatase (PTP) family, but because of two critical amino acid substitutions in the PTP domain are enzymatically inactive with standard PTP substrates. Recent studies, however, showed that IA-2β has low phosphatidylinositol phosphatase activity [9]. IA-2 is 979 and IA-2β is 986 amino acids in length. Both proteins are encoded by 23 exons and consist of an intracellular, transmembrane and luminal domain. They are 74% identical in their intracellular domain, but only 26% identical in their luminal domain. In the mouse *Ia-2* (also known as *Ptprn*) and *Ia-2β* (also known as *Ptprn2*) are located on chromosomes 1 and 12, respectively [10].

To elucidate the biological properties of IA-2 and IA-2β, we made single knockout (SKO) mice lacking either the *Ia-2* or *Ia-2β* genes and double knockout (DKO) mice lacking both genes [11–13]. Studies on the phenotypes of these animals revealed a number of abnormalities, particularly in the DKO mice, such as glucose intolerance, female infertility, and abnormalities in behaviour, learning and circadian rhythm [8, 14, 15]. These abnormalities were shown to be due to alterations in the secretion of hormones and neurotransmitters.

Much of the information on how IA-2 and/or IA-2β affects the secretion of hormones and neurotransmitters comes from in vitro experiments using hormone-secreting cell lines. Overproduction of IA-2 in MIN6 cells was found to increase insulin content and secretion of insulin, whereas the knockdown of IA-2 by RNAi decreased both content and secretion of insulin [16]. A key element in the secretory process was found to be the stability of DCV. These earlier experiments also showed that overproduction of IA-2 in MIN6 cells increased the half-life and number of DCV. However, the effect of the knockout of *Ia-2* and/or *Ia-2β* on the number of DCV in mice has not been studied. The present experiments were initiated to test the hypothesis that the knockout of these proteins in mice would result in a decrease in the half-life and number of DCV and that this, in turn, would affect the content and the secretion of insulin. We also documented alterations in the Ca^{2+} handling mechanisms of the beta cell in islets where *Ia-2*/*Ia-2β* is deleted.

Methods

Mice KO mice were prepared as described previously [11–13]. Because female $Ia\text{-}2^{-/-}/Ia\text{-}2\beta^{-/-}$ (DKO) mice are infertile [14], male DKO mice were bred to female $Ia\text{-}2^{-/-}/Ia\text{-}2\beta^{+/-}$ mice to generate DKO mice. Animals used in this study were produced in our institute animal core facility. All protocols were approved by the NIDCR Animal Care and Use Committee.

Islet isolation Islets from age- (3–4 months old) and sex-matched mice were isolated as described previously [17, 18]. Briefly, mice were anaesthetised by intraperitoneal injection with ketamine (50 mg/kg). Collagenase solution (Sigma, Saint Louis, MO, USA) was injected into the bile duct to inflate the pancreas. After digestion, islets were manually selected and washed in Krebs–Ringer HEPES buffer, and cultured overnight in RPMI-1640 medium (Invitrogen, Carlsbad, CA, USA) before further experiments.

Electron microscopy Isolated islets were fixed, sectioned [18, 19] and analysed at a primary beam voltage of 120 kV using a CM120 transmission electron microscope (FEI, Hillsboro, OR, USA) and a Gatan cooled 1k×1k CCD camera (Gatan, Pleasanton, CA, USA). Images were recorded with Digital Micrograph (Gatan) and montaged to evaluate the overall organisation of single cells. Each image was quantified by three individuals. Total DCV and lysosomal numbers and the number of DCVs below the plasma membrane were determined using NIH ImageJ.

Two-photon excitation imaging of exocytosis Exocytosis of DCVs was visualised in living islets with a solution containing the fluid-phase tracer sulforhodamine B (0.7 mmol/l) and two-photon excitation imaging [20, 21]. Exocytosis in response to 20 mmol/l glucose was measured within an arbitrary area (800 μm^2) of the islets. Imaging was acquired at 1 Hz using an inverted, laser-scanning microscope (FV1000 and I × 81, Olympus, Tokyo, Japan) equipped with a water-immersion objective (UPlanA-

po60xW/IR; N.A. 1.2, Olympus) and a femtosecond laser (MaiTai, Spectra Physics, Mountain View, CA, USA). Sites of exocytosis were detected manually.

Electrophysiological studies Details of measurements of intracellular free Ca^{2+} concentration [22, 23], voltage-gated Ca^{2+} current [22, 23] and membrane capacitance of beta cells [24] are provided in the electronic supplementary material (ESM).

Insulin content and secretion Groups of 25 islets on a 62 μm monofilament nylon mesh inside 13 mm Swinnex chambers (Millipore, Bedford, MA, USA) were perifused at 0.5 ml/min with KRB buffer containing 2.8 or 16.7 mmol/l glucose. Aliquots of perfusate (0.5 ml) were collected at different times over 1 h and stored at −80°C for measurements (Insulin RIA kit, Linco, St Charles, MO, USA). Insulin content in acidic alcohol-extracted islets was determined by RIA. Proinsulin content was determined by ELISA with antimouse proinsulin antibody CCI-17 (HyTest, Turku, Finland). Total protein level was measured by the MicroBCA Protein Assay (Pierce, Rockford, IL, USA).

Cathepsin D Two hundred freshly isolated islets were washed in Hanks' balanced salt solution and dissolved by sonication in 200 μl acetate-EDTA buffer (1.1 mmol/l EDTA, 5 mmol/l acetate, pH 5.0). Aliquots were used to determine lysosomal enzyme activity using a Cathepsin D Assay Kit (Sigma).

Autophagy Islets were cultured overnight before infection with adenovirus-GFP or LC3::GFP (gift from C. Miranti, Van Andel Research Institute, Grand Rapids, MI, USA). Control cells were infected with GFP alone (Ad-GFP). Islet cells were infected for 24 h before washing and cultured for an additional 24 h. Immunofluorescence with LC3 antibody (Clone 4E12; MBL, Woburn, MA, USA) was detected by confocal microscopy (Leica TCS SP2 microscope, Wetzlar, Germany). To quantify the extent of autophagy, the number of LC3::GFP punctate in each cell was counted using MetaMorph software (Molecular Devices).

Results

Insulin content and secretion To evaluate the effect of the KO of *Ia-2*, *Ia-2β* and both *Ia-2* and *Ia-2β* on insulin content, pancreatic islets were isolated and the amount of insulin in islet lysates was determined. As seen in Fig. 1a, the KO of *Ia-2*, *Ia-2β* and both *Ia-2* and *Ia-2β* resulted, respectively, in a 17%, 32% and 40% decrease in islet insulin content compared with wild-type (WT) mice ($p<0.01$). The decrease in insulin content resulted in a decrease in glucose-stimulated insulin secretion. Thus, when basal glucose was raised from 1.0 to 16.7 mmol/l, insulin secretion from the *Ia-2* KO, *Ia-2β* KO and DKO islets, measured 60 min later, was decreased by 32%, 31.5% and 57%, respectively, as compared with WT (Fig. 1b). The maximum decrease in insulin secretion (Fig. 1d) occurred during the first 10 min (Phase I) as compared with the next 50 min (Phase II, Fig. 1e) after raising glucose from 1.0 mmol/l to16.7 mmol/l. Although insulin content and the total amount of insulin secreted were significantly reduced in the KO mice, the fractional secretion of insulin (amount secreted divided by the total amount present) was only significantly different in the DKO mice (Fig. 1c). Further analysis showed that the fractional secretion of insulin in DKO mice was significantly lower in Phase I (ESM Fig. 1a), but not in Phase II (ESM Fig. 1b) compared with WT mice.

Number of DCV To determine whether the decrease in insulin content was due to a decrease in the number of DCV in the beta cells, a total of 26 beta cells from each of the four genotypes was evaluated by electron microscopy using NIH ImageJ software. A marked decrease in the number of DCV in the beta cells of *Ia-2* KO (1.48±0.10 vesicles/μm^2), *Ia-2β* KO (1.52±0.14 vesicles/μm^2) and DKO (0.56±0.03 vesicles/μm^2) mice was observed as compared with WT mice (3.15±0.14 vesicles/μm^2) (Fig. 2a–e) ($p<0.001$). The relative number of DCVs in beta cells of *Ia-2* KO, *Ia-2β* KO and DKO mice below the plasma membrane (100–400 nm) was significantly lower than that in WT (Fig. 2f). In the near docked shell (50–100 nm), the number of DCV in the DKO mice was much lower than in the other three groups. But in the docked shell (<50 nm), the DCV number in each of the four groups was very similar. No gross abnormalities were found in vesicle morphology or their degree of filling with cargo.

DCV exocytosis Two different methods were used to compare exocytotic events in KO and WT mice. The first method employed two-photon microscopy to image the fluorescent dye sulforhodamine B, which in principle is only taken up by beta cells during exocytosis due to the opening of DCV fusion pores (Fig. 3a). Red spots corresponding to DCV are then only briefly visualised when the DCV membrane fuses with the plasma membrane, after which the red spots disappear [20]. The number of transient fluorescent spots, which represent the occurrence of exocytosis, is then counted after stimulation with glucose. As seen in Fig. 3b, by this method exocytotic events were reduced by approximately 80% in the DKO mice as compared with WT ($p<0.01$).

The second method used to assess exocytosis involved monitoring changes in membrane capacitance in single

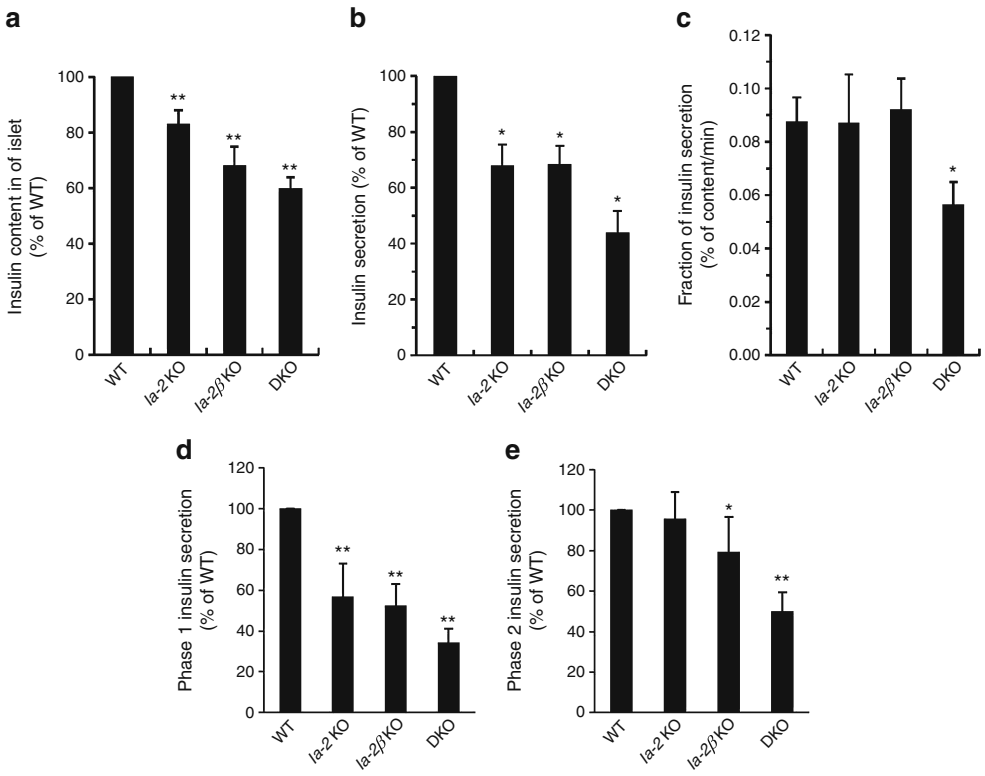

Fig. 1 Insulin content and glucose-stimulated insulin secretion in KO mice. **a** Insulin content in islets of KO mice compared with WT mice. **b** Glucose-stimulated insulin secretion determined 60 min after raising the glucose level from 1.0 to 16.7 mmol/l. **c** Fractional secretion of insulin (amount secreted divided by the total amount present). Glucose-stimulated insulin secretion in Phase I (**d**) compared with (**e**) Phase II. *$p<0.05$; **$p<0.01$. Columns (mean±SE) represent the average of five independent experiments, each genotype consisting of 25 islets performed in triplicate

mouse beta cells using the patch clamp technique. Under voltage clamp conditions, and with high glucose (11.1 mmol/l), membrane capacitance of beta cells isolated from WT mice increased following the application of brief depolarising pulses that trigger Ca^{2+} influx, and concomitantly increase DCV release. In contrast, the membrane capacitance of beta cells isolated from DKO mice was significantly decreased as compared with the beta cells of WT mice ($p<0.05$). Beta cells from *Ia-2 KO* and *Ia-2β* KO mice also showed decreased capacitance compared with beta cells from WT mice. A summary of these results is shown in Fig. 3d. Decreased capacitance is consistent with the reduced insulin content of islets of the knockout mice, and a reduced number of DCV. Thus, it appears that not only is the insulin content decreased and the numbers of DCV reduced, but this reduction extends to the readily releasable pool of granules that are secreted early on and are mainly assayed by the capacitance technique we used.

Previously we suggested [25] that the deletion of both *Ia-2* and *Ia-2β* had only a mild impact on intracellular $[Ca^{2+}]_i$. In the present study we measured changes in intracellular $[Ca^{2+}]_i$ in islets from WT, *Ia-2* KO, *Ia-2β* KO and DKO mice (representative tracings are shown in Fig. 4). In the WT islets, $[Ca^{2+}]_i$ was low and stable in 2.8 mmol/l glucose, the basal condition, but then increased to an early peak followed by regular oscillations when glucose was raised to 11.1 mmol/l. In islets from *Ia-2* KO, *Ia-2β* KO and DKO mice, the amplitude of the initial $[Ca^{2+}]_i$ peak at high glucose was reduced. Thus, although there was an 89.9±4.6% increase in $[Ca^{2+}]_i$ in WT islets, this increase was reduced to 66.6±7.81%, 59±4.3% and 38.2±5.4% in the *Ia-2* KO, *Ia-2β* KO, and DKO mouse islets respectively ($n=11$–18; $p<0.05$ vs WT for all groups). Although islets obtained from all of the mice showed $[Ca^{2+}]_i$ oscillations in 11.1 mmol/l glucose, the steady-state frequency of these oscillations was significantly greater in the WT compared with the DKO mice. Also in the steady state, baseline-subtracted peak $[Ca^{2+}]_i$ trended towards lower values in KO vs WT islets, with changes in ratio being 0.47±0.03 vs 0.54±0.05, respectively (mean±SEM; $n=17$–25 islets), although these differences were not significant ($p>0.05$).

To assess whether these changes in $[Ca^{2+}]_i$ or possibly secretion might reflect reduced activation of voltage-dependent Ca^{2+} currents in beta cells from the KO animals, we measured Ca^{2+} currents in isolated beta cells using standard approaches [23]. In mouse beta cells, most of the Ca^{2+} influx coupled to insulin granule release is mediated by dihydropyridine-sensitive or 'L-type' Ca^{2+} channels, although other Ca^{2+} channels also contribute to the total Ca^{2+} influx [26–28]. We found that beta cell Ca^{2+} currents were substantially decreased in amplitude in the DKO beta cells as compared with the SKOs or WT mice (Fig. 4e). These results suggest that reduced Ca^{2+} influx is likely to

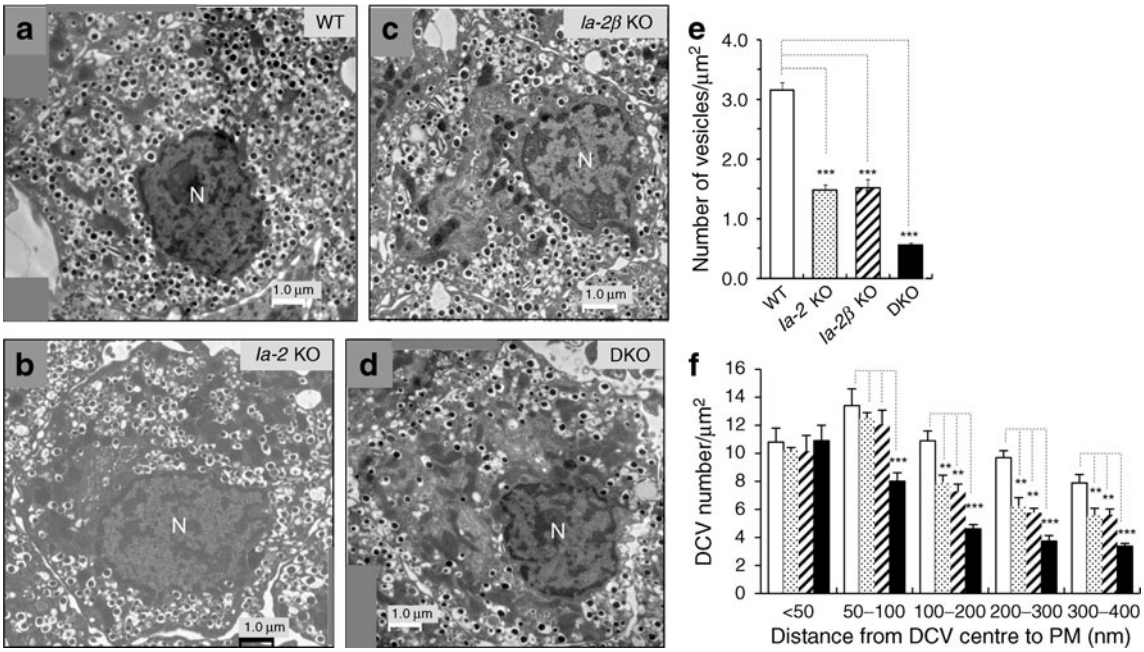

Fig. 2 Number of DCV in WT and KO mice. Representative electron micrographs showing DCV in beta cells of (**a**) WT, (**b**) *Ia-2* KO, (**c**) *Ia-2β* KO and (**d**) DKO mice. Scale bars, 1 µm. **e** Analysis of DCV from 26 beta cells from each of the four genotypes (three mice per genotype). **f** Relative density of DCVs located in 50 or 100 nm concentric shells in the first 400 nm below the plasma membrane (PM) was plotted (n=26 beta cells in each group). In the readily releasable pool (<200 nm), the average densities of DCVs (number/µm^2±SE) in *Ia-2* KO (9.67±0.77), *Ia-2β* KO (9.24±0.64) and DKO beta cells (7.07±0.44) are significantly lower than that in WT (11.51±0.64) (p<0.05, p<0.05, and p<0.0001 respectively). Each electron micrograph was quantified by three individuals and analysed by NIH ImageJ software. **p<0.01; ***p<0.001 (mean±SE). White bars, WT; dotted bars, *Ia-2 KO*; hatched bars, *Ia-2β* KO; black bars, DKO

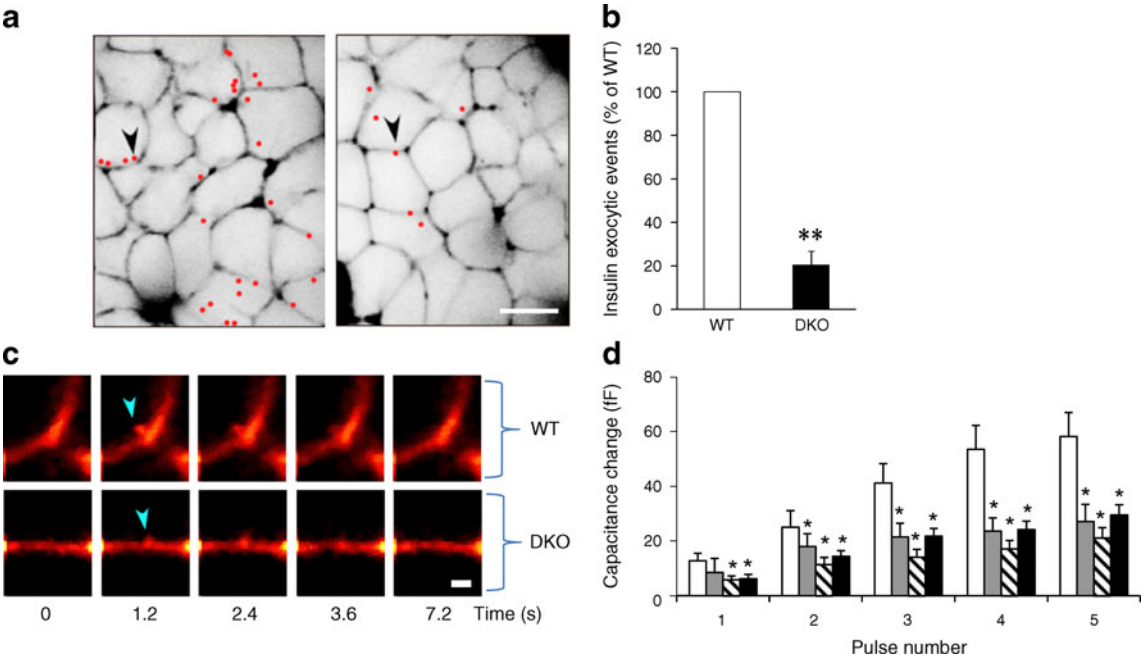

Fig. 3 Glucose-stimulated DCV exocytosis in islets evaluated by two-photon microscopy. **a** Spatial distribution of exocytotic sites in the islet cells: Left, WT, right, DKO. Scale bar, 10 µm. **b** Quantification of insulin exocytotic events. **p<0.01. **c** Single exocytotic events visualised with polar fluorescent tracer, the red fluorescence dye sulforhodamine B (SRB). Transient red spots disappear at the moment of exocytosis and represent secretion of insulin. Scale bar, 1 µm. **d** Mean increases in capacitance elicited by membrane depolarisation were significantly less in KO than WT mice. *p<0.05. The capacitances for each group tested were determined using 5–16 beta cells. Error bars show standard error of the mean. White bars, WT; grey bars, *Ia-2* KO; hatched bars, *Ia-2β* KO; black bars, DKO

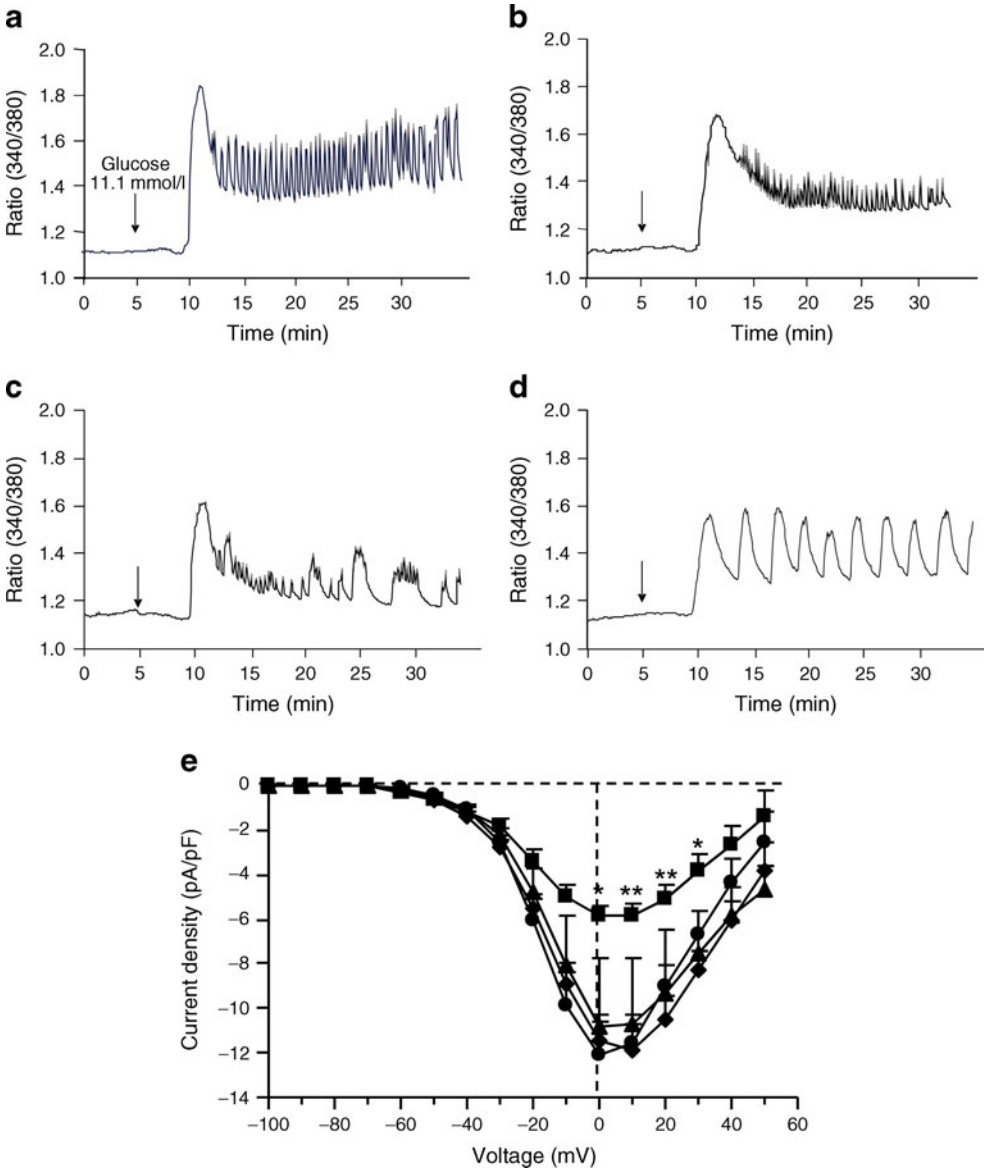

Fig. 4 Changes in glucose-dependent islet $[Ca^{2+}]_i$ oscillations and voltage-dependent Ca^{2+} currents in WT and KO. **a** The first peak in $[Ca^{2+}]_i$ seen upon raising glucose from 2.8 to 11.1 mmol/l was higher, and the steady-state frequency as well as the regularity of the $[Ca^{2+}]_i$ oscillations were greater in WT vs KO mice (**a** WT; **b** *Ia-2* KO; **c** *Ia-2β* KO; **d** DKO). **e** Under voltage clamp conditions, there was also a substantial decrease in the voltage-dependent Ca^{2+} currents of beta cells from DKO compared with beta cells from SKO or WT mice. Ca^{2+} currents were evoked using 40 ms clamp commands from −100 to +60 mV from a holding potential of −65 mV (see "Methods"). The numbers of beta cells used for the whole-cell calcium measurements were 10, 6, 6 and 13 for WT, *Ia-2* KO, *Ia-2β* KO, and DKO respectively. Error bars show SEM. Squares, DKO; circles, *Ia-2* KO; diamonds, WT; triangles, *Ia-2β* KO

have contributed to the reduced initial rise in $[Ca^{2+}]_i$ observed in the DKO beta cells [25]. Thus, loss of *Ia-2* and *Ia-2β* may decrease secretion not only via a decrease in the number of beta cell DCVs, but because reduced Ca^{2+} influx leads to the release of a smaller fraction of an already smaller pool of releasable granules, reducing the exocytotic rate. This could help account for the decreased glucose-stimulated insulin secretion seen even after normalisation for decreased insulin content in islets from DKO animals.

Half-life of DCV As most of the insulin within beta cells is stored within DCV, the half-life of insulin is a surrogate of DCV stability [16]. To investigate the possibility that the decrease in the number of insulin-containing vesicles in the KO mice was due to a decrease in the stability of the DCV as a result of the KO of *Ia-2* and/or *Ia-2β*, the half-life of insulin was measured. As seen in Fig. 5a, the half-life of the DCV from the DKO, *Ia-2* KO and *Ia-2β* KO mice was 21, 26 and 72 h, respectively, compared with 96 h for the DCV of the WT mice. The value for the WT mice is in the range reported in the literature for other WT mice (72–120 h). Thus, the half-life of DCV from the DKO and *Ia-2* KO mice is about one-quarter of that of the WT mice. To be certain that the decreased half-life of the DCV in the KO mice was not the result of a decrease in the biosynthesis of proinsulin, isolated islets were pulsed with [^{35}S]methionine and [^{35}S]cysteine and the level of newly synthesised proinsulin was determined. During the first 30 min, newly synthesised proinsulin was 25%, 40% and 60% higher in *Ia-2* KO, *Ia-2β* KO and DKO islets, respectively, than in WT islets (ESM Fig. 2a). At the end of a 90–150 min

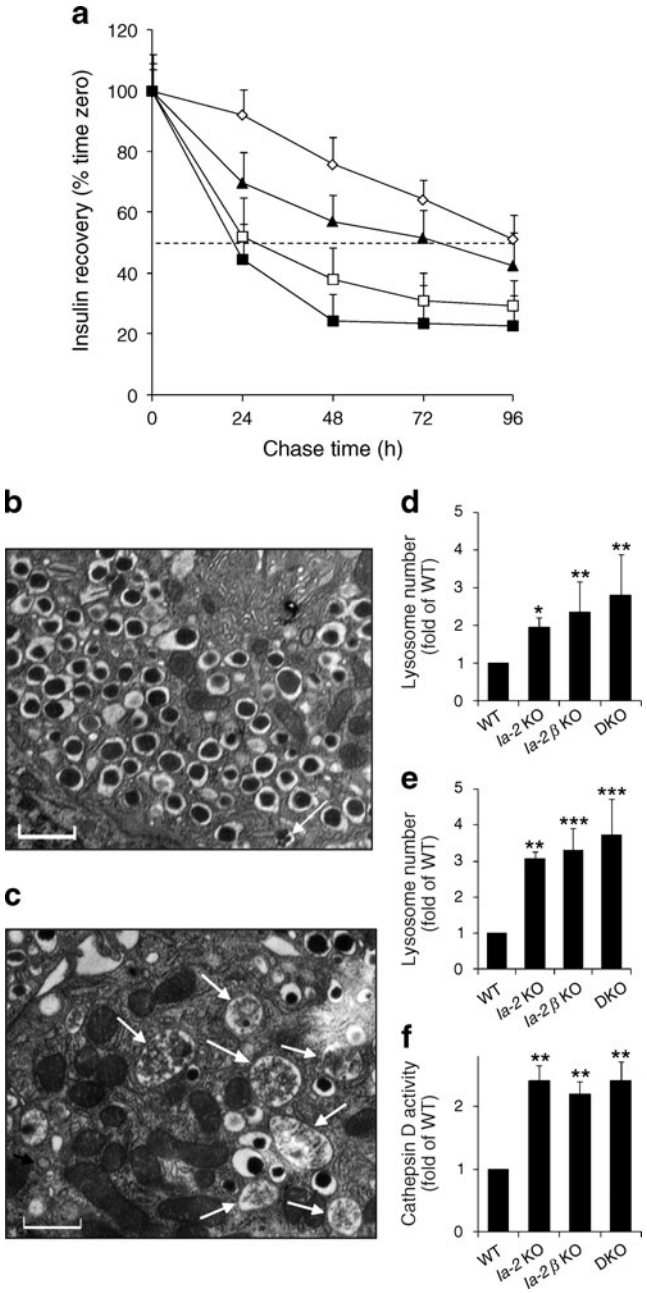

Fig. 5 Half-life of DCV. **a** Islets were pulsed with [^{35}S]methionine and [^{35}S]cysteine and chased for 96 h. Labelled insulin was pulled down with anti-insulin antibody and the half-life of insulin in the WT and KO islets was determined. WT vs DKO mice, $^{**}p<0.01$. White diamonds, WT; black triangles, *Ia-2β* KO; white squares, *Ia-2* KO; black squares, DKO; triangles, **b**, **c** Lysosomes in beta cells of mice. Representative electron micrographs showing a substantial increase in the number and size of lysosomes (white arrows) in the beta cells of the DKO as compared with the WT mice. Scale bars, 100 mm. **d** Lysosome number; **e** lysosome size; and **f** cathepsin D activity in the islets. $^{*}p<0.05$, $^{**}p<0.01$, $^{***}p<0.001$

pulse, the amount of proinsulin synthesised in the islets of the KO mice was equal to or slightly greater than the amount synthesised in the islets of the WT mice. Transcript levels of preproinsulin genes 1 and 2 were increased ~20% in the *Ia-2* KO and *Ia-2β* KO islets and ~50% in DKO islets, compared with WT islets (ESM Fig. 2b). This argues that the decreased half-life of the DCV in the KO mice was not due to impairment in the biosynthesis of insulin.

Lysosomes The finding that the number and half-life of DCV was significantly decreased in the KO mice, suggested that the reduction of DCV number could be the result of accelerated DCV degradation. To examine the effect of the KO of *Ia-2* and/or *Ia-2β* on lysosomes, we measured the number and size of the lysosomes in the WT and KO mice (Fig. 5b, c). The average number of lysosomes in the beta cells of *Ia-2* KO, *Ia-2β* KO and DKO mice compared with WT mice was increased 2.0–2.8-fold per 39 μm^2 cytosolic areas (Fig. 5d). The average size of these lysosomes in the *Ia-2* KO, *Ia-2β* KO and DKO beta cells was increased 3.0–3.7-fold as compared with the lysosomes of WT mice (Fig. 5e). In addition to the increase in the number and size of the lysosomes, cathepsin D, a lysosomal associated enzyme, was increased 2.2–2.4-fold in the KO compared with the WT mice ($p<0.01$) (Fig. 5f).

Autophagy To see if the decrease in the number and half-life of the DCV might be related to lysosome-mediated destruction [29–31], beta cells of WT and KO mice were examined by electron microscopy. Fig. 6a–c shows the fusion and uptake of DCV by lysosomes. Autophagic activity also was evaluated by quantifying the autophagic marker LC3, which conjugates to lipid molecules on autophagic membranes. Isolated islet cells, transfected with adenovirus-LC3-GFP, showed that LC3-GFP aggregates (punctate) were markedly increased in KO islets (Fig. 6e–g) compared with WT islets (Fig. 6d). Quantitative analysis revealed 2.8-, 2.4- and 6.9-fold increases of LC3-GFP, respectively, in *Ia-2* KO, *Ia-2β* KO and DKO mice (Fig. 6h). These findings indicate that autophagocytic activity is markedly upregulated in KO islets.

Discussion

The present study shows that the KO of *Ia-2* and/or *Ia-2β* results in a marked decrease in the number of DCV in beta cells and a decrease in beta cell $[Ca^{2+}]_i$ handling. In the case of the SKO mice, the decrease in the insulin content of the beta cells and the decrease in insulin secretion correlate roughly with the decrease in the number of DCV. In the case of the DKO mice, the decrease in the number of DCV is proportionally greater than the decrease in insulin content and secretion (Figs 1 and 2). One possible explanation for the apparent discrepancy is that undigested

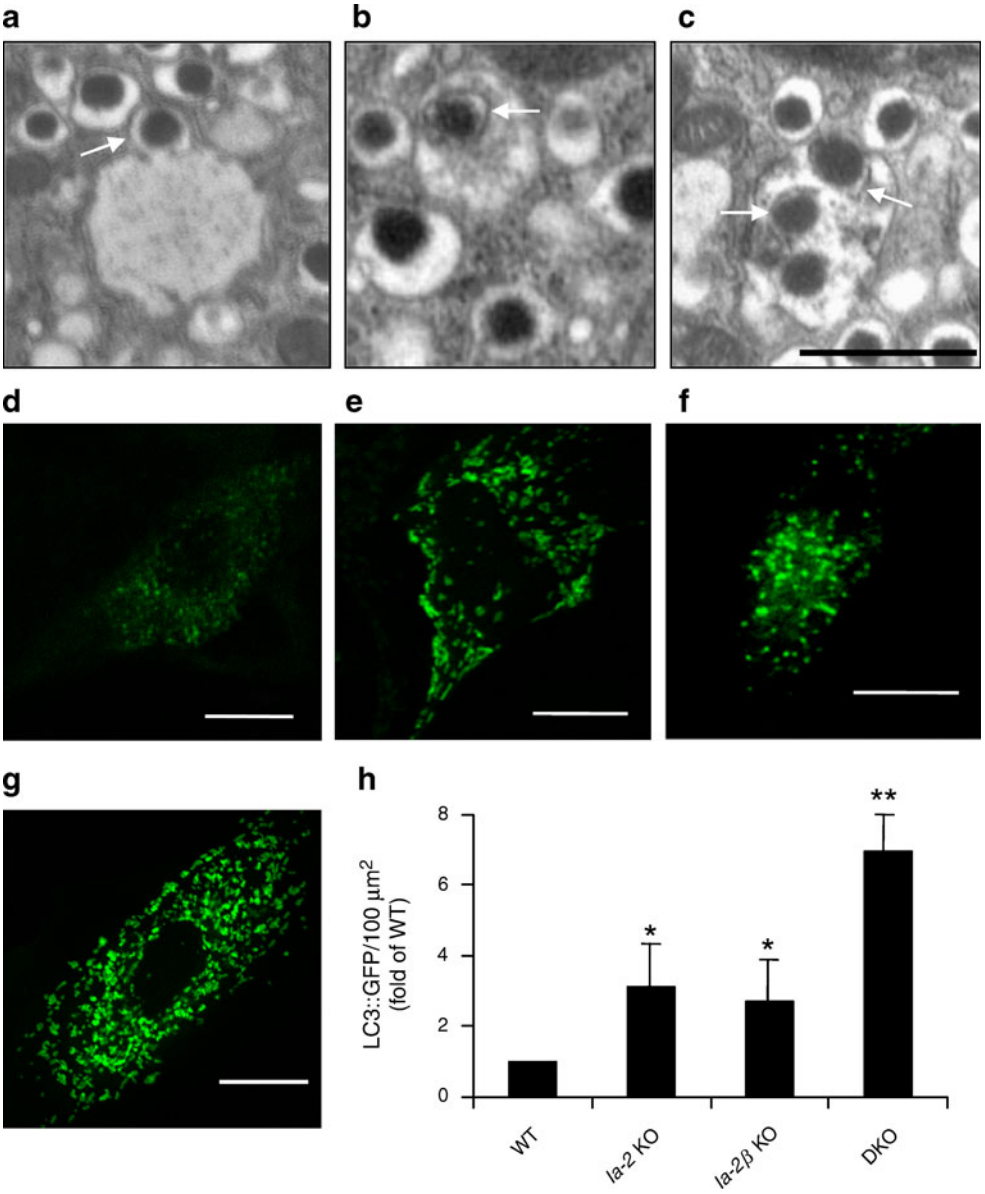

Fig. 6 Representative electron micrographs of beta cells showing (**a**) fusion and (**b**) uptake of DCV by lysosomes and (**c**) by multigranular bodies (scale bar, 1 μm) in *Ia-2* KO, *Ia-2β* KO and DKO mice respectively. Cultured islet cells from WT and KO mice (**d**–**g**) transfected with adenovirus-LC3::GFP showing an increase in the conjugation of LC3::GFP to autophagic membranes of the KO compared with the WT mice. Scale bars, 10 μm. **h** Quantificative analysis of LC3-GFP in each of the genotypes. *$p<0.05$; **$p<0.01$

or partially digested granules in autophagosomes and lysosomes, which contained some of the measurable insulin molecules, falsely inflated the amount of insulin attributed to the vesicles.

The capacitance experiments revealed that the expected membrane changes, induced experimentally by depolarising pulses, were reduced in the KO beta cells. This is consistent with the decrease in the total number of DCVs and a decrease in the number of readily releasable vesicles. Considering that the number of the docked DCVs (<50 nm) was essentially the same in four groups, the diminished Phase I secretion in KO beta cells may in part be secondary to the effect of the KO of *Ia-2/Ia-2β* on the Ca^{2+} signalling pathway. As insulin secretion measured from islets is the product of the number of granules available for release and the release probability of the individual granules, secretion can be reduced physiologically by decreasing either the number of vesicles or the rate of exocytosis or both. In this context, it is of interest that whereas in the present study there was a significant decrease in the fractional secretion of insulin (i.e. amount secreted divided by total amount present) in beta cells of DKO mice (Fig. 1c), no such decrease was found in our earlier study [25]. This may be due to the fact that much older animals (13–18 months old) were used in the earlier study as compared with the younger animals (4–6 months old) in the present study. One possible explanation is that nearly 50% of the DKO mice die by 40 weeks of age compared with few, if any, of the WT mice [8]. This raises the possibility that the older DKO survivors might be more resistant to changes in insulin secretion.

Our findings also suggest that the pronounced decrease in exocytotic events in KO mice, as determined by two-photon microscopy and patch clamp capacitance measurements, is most likely secondary to the pronounced decrease in the number of DCV. In this context, only in the DKO mice was the amplitude of the voltage-gated L type Ca^{2+} current, which would be expected to cause the release of less DCV upon beta cell stimulation, significantly reduced (Fig. 4b). Whether this is an important contributing factor to the greater reduction of exocytosis in the DKO mice as compared with the SKO mice remains to be determined. It would be of considerable interest if the KO of *Ia-2* and/or *Ia-2β* in turn altered Ca^{2+} channel activity, as vesicle proteins and Ca^{2+} channels are known to form a dynamic complex in secretory cells, including beta cells, and these can regulate the channels [32–35]. We also found that loss of *Ia-2/Ia-2β* had a significant modulatory action on islet Ca^{2+} oscillations, such that the frequency of the oscillations was reduced in the DKO islets. We also found that the initial Ca^{2+} level obtained on increasing glucose from 2.8 to 11.1 mmol/l was reduced in the KO islets, although the relationship between these changes and those in the amplitude of the voltage-gated Ca^{2+} currents remains to be elucidated in detail.

Previously, we suggested that IA-2 affects the stability of DCV [16]. This was based on the observation that overproduction of IA-2 in MIN6 cells (Fig. 7) resulted in an almost twofold increase in the half-life of the DCV and approximately a 2.5-fold increase in the number of DCV. This, in turn, led to an increase in the content and secretion of insulin. However, the effect of the knockdown in MIN6 cells or the knockout in mice of *Ia-2* and/or *Ia-2β* on the number and half-life of DCV was not determined. In *Caenorhabditis elegans*, we found that the deletion of *Ia-2* homologue gene *Ida-1* resulted in a significant decrease in the number of DCVs in neuronal cells, but the deletion did not have a negative effect on insulin mRNA levels or the Stat signalling pathway [36], a possibility proposed by others [37]. The current KO experiments in mice add strong support to the idea that *Ia-2* and *Ia-2β* have a profound effect on the stability (half-life) of DCV (Fig. 7).

The decrease in DCV half-life appears to be the most likely explanation for the decrease in DCV number and mechanistically may be related to the observed increase in the number and size of lysosomes (Fig. 5). The DCV of the KO mice may be recognised by the lysosomes as abnormal and this, in turn, could lead to their destruction by crinophagy and/or autophagy [29–31]. However, it is possible that the abnormal DCV of the KO mice may self-destruct and the increase in crinophagy and autophagy could simply represent an attempt by the cell to rid itself of abnormal DCV and related degraded proteins. At present we cannot differentiate between these two possibilities. Although by electron microscopy we found evidence for both crinophagy and autophagy, the significant increase (2.8- to 6.9-fold) in the binding of LC3:GFP (Fig. 6d–h) to islets of both SKO and DKO mice argues in favour of autophagy by providing quantificative support for the importance of this process.

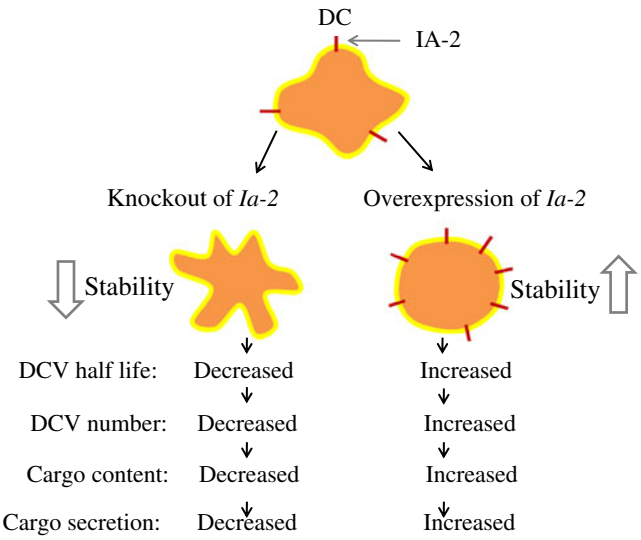

Fig. 7 Effect of IA-2 on the stability of DCV. In mice, the KO of *Ia-2* destabilises and decreases the half-life of DCV. In turn, the number of DCV, the amount of insulin in beta cells and its secretion, is decreased. In MIN6 cells, overproduction of IA-2 adds stability to and increases the half-life of DCV. In turn, the number of DCV, the amount of insulin in beta cells and its secretion is increased

DCV are found not only in islets, but also in neuroendocrine organs throughout the body, especially the brain. Recently we observed profound changes in the behaviour, learning ability and circadian rhythm (i.e. blood pressure, heart rate, body temperature and physical activity) in the DKO mice [8, 15]. These changes appear to be due to a decrease in the secretion of neurotransmitters. Although both IA-2 and/or IA-2β were initially thought to be primarily associated with DCV, we now know that IA-2β also is present in synaptic vesicles [8]. Thus, the findings in the DKO mice, which usually show a stronger phenotype than the single KO mice, may be the result of alterations in both DCV and synaptic vesicles.

There are dozens of membrane and transmembrane proteins associated with DCV [38]. Based on the findings with *Ia-2* and *Ia-2β* in mice and genetic association studies [39–42], it is not unreasonable to suggest that at the human level mutations in one or more of these many DCV proteins might lead to abnormalities (e.g. RAB27A, Griscelli syndrome [43]) in secretory function in other disorders such as diabetes.

Acknowledgements We thank C. Wohlenberg (NIDCR/NIH, Bethesda, MD, USA) for technical help. This research was supported in part by the Intramural Research Program of the NIH (NIDCR and NIBIB) and grant NIH RO1 DK46409 for the Satin laboratory. The authors thank A. Sherman (NIDDK/NIH, Bethesda, MD, USA) and M. Merrins (L.S. Satin's lab) for helpful discussions.

T.C., H.H., G.Z., M.Z., N.T., H.K., L.S.S., R.D.L. and A.L.N. conceived and designed the experiments. T.C., H.H., G.Z., M.Z., N.T. performed the experiments. T.C., H.H., G.Z., M.Z., N.T., H.K., L.S.S., R.D.L. and A.L.N analysed the data. T.C. and A.L.N. were responsible for drafting the paper. T.C., H.H., G.Z., M.Z., N.T., H.K., L.S.S., R.D.L. and A.L.N. revised and approved the final version of paper.

Duality of interest The authors declare that there is no duality of interest associated with this manuscript

References

1. Lan MS, Lu J, Goto Y, Notkins AL (1994) Molecular cloning and identification of a receptor-type protein tyrosine phosphatase, IA-2, from human insulinoma. DNA Cell Biol 13:505–514
2. Lu J, Li Q, Xie H et al (1996) Identification of a second transmembrane protein tyrosine phosphatase, IA-2beta, as an autoantigen in insulin-dependent diabetes mellitus: precursor of the 37-kDa tryptic fragment. Proc Natl Acad Sci USA 93:2307–2311
3. Notkins AL, Lernmark A (2001) Autoimmune type 1 diabetes: resolved and unresolved issues. J Clin Invest 108:1247–1252
4. Verge CF, Gianani R, Kawasaki E et al (1996) Prediction of type I diabetes in first-degree relatives using a combination of insulin, GAD, and ICA512bdc/IA-2 autoantibodies. Diabetes 45:926–933
5. Bingley PJ, Bonifacio E, Gale EA (1993) Can we really predict IDDM? Diabetes 42:213–220
6. Kulmala P, Savola K, Petersen JS et al (1998) Prediction of insulin-dependent diabetes mellitus in siblings of children with diabetes. A population-based study. The Childhood Diabetes in Finland Study Group. J Clin Invest 101:327–336
7. Solimena M, Dirkx R Jr, Hermel JM et al (1996) ICA 512, an autoantigen of type I diabetes, is an intrinsic membrane protein of neurosecretory granules. EMBO J 15:2102–2114
8. Nishimura T, Kubosaki A, Ito Y, Notkins AL (2009) Disturbances in the secretion of neurotransmitters in IA-2/IA-2beta null mice: changes in behavior, learning and lifespan. Neuroscience 159:427–437
9. Caromile LA, Oganesian A, Coats SA, Seifert RA, Bowen-Pope DF (2010) The neurosecretory vesicle protein phogrin functions as a phosphatidylinositol phosphatase to regulate insulin secretion. J Biol Chem 285:10487–10496
10. Cai T, Krause MW, Odenwald WF, Toyama R, Notkins AL (2001) The IA-2 gene family: homologs in *Caenorhabditis elegans*, *Drosophila* and zebrafish. Diabetologia 44:81–88
11. Saeki K, Zhu M, Kubosaki A, Xie J, Lan MS, Notkins AL (2002) Targeted disruption of the protein tyrosine phosphatase-like molecule IA-2 results in alterations in glucose tolerance tests and insulin secretion. Diabetes 51:1842–1850
12. Kubosaki A, Gross S, Miura J et al (2004) Targeted disruption of the IA-2beta gene causes glucose intolerance and impairs insulin secretion but does not prevent the development of diabetes in NOD mice. Diabetes 53:1684–1691
13. Kubosaki A, Nakamura S, Notkins AL (2005) Dense core vesicle proteins IA-2 and IA-2beta: metabolic alterations in double knockout mice. Diabetes 54(Suppl 2):S46–S51
14. Kubosaki A, Nakamura S, Clark A, Morris JF, Notkins AL (2006) Disruption of the transmembrane dense core vesicle proteins IA-2 and IA-2beta causes female infertility. Endocrinology 147:811–815
15. Kim SM, Power A, Brown TM et al (2009) Deletion of the secretory vesicle proteins IA-2 and IA-2beta disrupts circadian rhythms of cardiovascular and physical activity. FASEB J 23:3226–3232
16. Harashima S, Clark A, Christie MR, Notkins AL (2005) The dense core transmembrane vesicle protein IA-2 is a regulator of vesicle number and insulin secretion. Proc Natl Acad Sci USA 102:8704–8709
17. Gotoh M, Maki T, Kiyoizumi T, Satomi S, Monaco AP (1985) An improved method for isolation of mouse pancreatic islets. Transplantation 40:437–438
18. Zhang G, Hirai H, Cai T et al (2007) RESP18, a homolog of the luminal domain IA-2, is found in dense core vesicles in pancreatic islet cells and is induced by high glucose. J Endocrinol 195:313–321
19. Goping G, Pollard HB, Srivastava M, Leapman R (2003) Mapping protein expression in mouse pancreatic islets by immunolabeling and electron energy loss spectrum-imaging. Microsc Res Tech 61:448–456
20. Takahashi N, Kishimoto T, Nemoto T, Kadowaki T, Kasai H (2002) Fusion pore dynamics and insulin granule exocytosis in the pancreatic islet. Science 297:1349–1352
21. Takahashi N, Hatakeyama H, Okado H et al (2004) Sequential exocytosis of insulin granules is associated with redistribution of SNAP25. J Cell Biol 165:255–262
22. Zhang M, Goforth P, Bertram R, Sherman A, Satin L (2003) The Ca^{2+} dynamics of isolated mouse beta-cells and islets: implications for mathematical models. Biophys J 84:2852–2870
23. Kinard TA, Satin LS (1996) Temperature modulates the Ca^{2+} current of HIT-T15 and mouse pancreatic beta-cells. Cell Calcium 20:475–482
24. Horrigan FT, Bookman RJ (1994) Releasable pools and the kinetics of exocytosis in adrenal chromaffin cells. Neuron 13:1119–1129
25. Henquin JC, Nenquin M, Szollosi A, Kubosaki A, Louis Notkins A (2008) Insulin secretion in islets from mice with a double knockout for the dense core vesicle proteins islet antigen-2 (IA-2) and IA-2{beta}. J Endocrinol 196:573–581
26. Yang SN, Berggren PO (2006) The role of voltage-gated calcium channels in pancreatic beta-cell physiology and pathophysiology. Endocr Rev 27:621–676
27. Tian Y, Corkey RF, Yaney GC, Goforth PB, Satin LS, Moitoso de Vargas L (2008) Differential modulation of L-type calcium channel subunits by oleate. Am J Physiol Endocrinol Metab 294:E1178–E1186
28. Mears D (2004) Regulation of insulin secretion in islets of Langerhans by Ca(2+)channels. J Membr Biol 200:57–66
29. Mizushima N, Levine B, Cuervo AM, Klionsky DJ (2008) Autophagy fights disease through cellular self-digestion. Nature 451:1069–1075
30. Marsh BJ, Soden C, Alarcon C et al (2007) Regulated autophagy controls hormone content in secretory-deficient pancreatic endocrine beta-cells. Mol Endocrinol 21:2255–2269
31. Speidel D, Salehi A, Obermueller S et al (2008) CAPS1 and CAPS2 regulate stability and recruitment of insulin granules in mouse pancreatic beta cells. Cell Metab 7:57–67

32. Wiser O, Trus M, Hernandez A et al (1999) The voltage sensitive Lc-type Ca^{2+} channel is functionally coupled to the exocytotic machinery. Proc Natl Acad Sci USA 96:248–253
33. Ji J, Muinuddin A, Kang Y, Diamant NE, Gaisano HY (2003) SNAP-25 inhibits L-type Ca^{2+} channels in feline esophagus smooth muscle cells. Biochem Biophys Res Commun 306:298–302
34. Nunemaker CS, Bertram R, Sherman A, Tsaneva-Atanasova K, Daniel CR, Satin LS (2006) Glucose modulates $[Ca^{2+}]_i$ oscillations in pancreatic islets via ionic and glycolytic mechanisms. Biophys J 91:2082–2096
35. Trus M, Corkey RF, Nesher R et al (2007) The L-type voltage-gated Ca^{2+} channel is the Ca^{2+} sensor protein of stimulus-secretion coupling in pancreatic beta cells. Biochemistry 46:14461–14467
36. Cai T, Hirai H, Fukushige T et al (2009) Loss of the transcriptional repressor PAG-3/Gfi-1 results in enhanced neurosecretion that is dependent on the dense-core vesicle membrane protein IDA-1/IA-2. PLoS Genet 5:e1000447
37. Mziaut H, Trajkovski M, Kersting S et al (2006) Synergy of glucose and growth hormone signalling in islet cells through ICA512 and STAT5. Nat Cell Biol 8:435–445
38. Brunner Y, Coute Y, Iezzi M et al (2007) Proteomics analysis of insulin secretory granules. Mol Cell Proteomics 6:1007–1017
39. Chernysheva A, Tsitlidze NM, Savost'ianov KV et al (2008) Association of the chromosomal region 2q35 with type 1 diabetes mellitus in the Russian patients from Moscow. Genetika 44:232–235
40. Yang JH, Downes K, Howson JM et al (2011) Evidence of association with type 1 diabetes in the SLC11A1 gene region. BMC Med Genet 12:59
41. An P, Freedman BI, Hanis CL et al (2005) Genome-wide linkage scans for fasting glucose, insulin, and insulin resistance in the National Heart, Lung, and Blood Institute Family Blood Pressure Program: evidence of linkages to chromosome 7q36 and 19q13 from meta-analysis. Diabetes 54:909–914
42. Schelling JR, Abboud HE, Nicholas SB et al (2008) Genome-wide scan for estimated glomerular filtration rate in multi-ethnic diabetic populations: the Family Investigation of Nephropathy and Diabetes (FIND). Diabetes 57:235–243
43. Menasche G, Pastural E, Feldmann J et al (2000) Mutations in RAB27A cause Griscelli syndrome associated with haemophagocytic syndrome. Nat Genet 25:173–176